Mon. Not. R. Astron. Soc. **000**, 000–000 (0000) Printed 1 February 2008 (MN LATEX style file v2.2)

The polarization in the JVAS/CLASS flat-spectrum radio sources: II. A search for aligned radio polarizations

S.A. Joshi, R.A. Battye, I.W.A. Browne, N. Jackson, T.W.B. Muxlow, and P.N. Wilkinson
The University of Manchester, Jodrell Bank Observatory, Macclesfield, Cheshire, SK11 9DL, U.K.

arXiv:0705.2548v1 [astro-ph] 17 May 2007

1 February 2008

ABSTRACT

We have used the very large JVAS/CLASS 8.4-GHz surveys of flat-spectrum radio sources to test the hypothesis that there is a systematic alignment of polarization position angle vectors on cosmological scales of the type claimed by Hutsemékers et al. (2005). The polarization position angles of 4290 sources with polarized flux density $\geq$1 mJy have been examined. They do not reveal large-scale alignments either as a whole or when split in half into high-redshift ($z \geq 1.24$) and low-redshift sub-samples. Nor do the radio sources which lie in the specific areas covered by Hutsemékers et al. (2005) show any significant effect. We have also looked at the position angles of parsec-scale jets derived from VLBI observations and again find no evidence for systematic alignments. Finally, we have investigated the correlation between the polarization position angle and those of the parsec-scale jets. As expected, we find that there is a tendency for the polarization angles to be perpendicular to the jet angles. However, the difference in jet and polarization position angles does not show any systematic trend in different parts of the sky.

Key words: polarization – surveys – galaxies:active

1 INTRODUCTION

In an isotropic universe the sizes of the largest coherent structures are expected to be limited by the time taken for the primordial density fluctuations to undergo gravitational collapse. In practice both observations of large-scale structures and the latest N-body simulations agree that the largest structures have scales of $\leq$100 Mpc. It is therefore obvious that any observation of coherent behaviour of objects on much larger scales than $\sim$100 Mpc would have profound implications for our understanding of the nature of the Universe. Over the years there have in fact been several reports of the detection of large-scale coherence, mostly based on measurements of the linear polarizations of active galaxies, and more recently based on observations of the cosmic microwave background (CMB).

Birch (1982) claimed to have found evidence for a rotating universe by comparing the radio polarization position angles for extended radio sources with the direction of elongation of radio sources. The claim was that there were systematic offsets between the two position angles and that these were systematically different in widely different part of the sky. Though attacked on statistical grounds at the time (e.g. Phinney & Webster 1983) it is not clear that this "Birch effect" has totally gone away (Kendall & Young 1984; Jain et al., 2003). An independent effect claimed by Nodland and Ralston (1997) was that there is a systematic rotation of plane of polarization over cosmological distances. But Wardle et al (1997) refute their claim by pointing out that in individual radio sources the polarization position angles are strongly correlated with extended radio morphology, even at high redshift which excludes large cosmological rotations. Also the Nodland and Ralston claim has been attacked on the basis of statistics (e.g. Carroll and Field (1997), Eisenstien and Bunn (1997), Loredo et al (1997)).

More recently, Hutsemékers (1998), Hutsemékers & Lamy (2001) and Hutsemékers et al. (2005) have been accumulating evidence that the linear polarizations of quasars in optical wavelengths are non-uniformly distributed, being systematically different near the North and South Galactic poles. They also find that the clustering of position angles is more evident if they divide their sample of 355 sources by redshift. They use this fact to argue against the effect being a result of the polarization of the quasar light as it passes through Galactic interstellar dust since this would affect all redshifts indiscriminately.

Stimulated by these hints of interesting polarization ef-

fects, and reports of a preferred axis in CMB fluctuations (Schwarz et al., 2004; Land & Magueijo, 2005; Raeth et al., 2007), we decided to examine some linear polarization measurements we had made with the Very Large Array (VLA) between 1990 and 1999 of a large sample of compact flat-spectrum radio sources. The JVAS (Jodrell Bank-VLA Astrometric Survey) programme from 1990-1992 (Patnaik et al. 1992, Browne et al. 1998, Wilkinson et al. 1998) was undertaken with the two main objectives of measuring accurate positions for sources to find interferometer phase calibrators and to identify gravitationally lensed sources. However, we also obtained data for the linear polarizations of the 2308 sources. In addition, the later CLASS survey (1994-1999; Myers et al. 2003, Browne et al. 2003) targeted fainter compact radio sources and the majority of these observations have suitable calibrators available to derive degrees of polarization. The total size of the JVAS/CLASS surveys is 16503 sources, and as we discuss in Jackson et al., (2007) (hereafter Paper I), 4290 have polarized flux density $\geq$1 mJy. These 4290 sources we make use of for studies of possible polarization alignments.

On its way to the observer polarized radiation passes both through the host galaxy of the AGN and the Galaxy and suffers Faraday rotation. Since it is dependent on the square of the wavelength, Faraday rotation is therefore a much more significant effect at radio than at optical wavelengths. However, as we have shown in Paper I, total rotation measures are generally much too small to destroy information about the intrinsic position angles of polarization when the measurements are made at 8.4 GHz.

2 INITIAL RESULTS AND REANALYSIS

Our initial examination of JVAS for evidence of aligned radio polarizations made use of the original calibrations of the data done primarily with astrometry in mind and not the accurate measurement of source polarizations. Using these data we did initially find apparent systematic alignments so we decided on a careful re-calibration of both the JVAS and CLASS data, concentrating on polarizations. The results of this recalibration and analysis are presented in Paper I.

2.1 The data and analysis

We make use of the 4290 sources presented in Paper I and full details of the calibration and analysis are given therein. See Fig. 1 for the Aitoff projection of the data. Here we only briefly address calibration and analysis issues which may be directly relevant to any search for systematic alignments of polarization position angles within the sample. These issues are:

• *Polarization residual calibration.* Incorrect removal of instrumental polarization residuals can lead to a bias in the measured polarization angles. The JVAS/CLASS observations were concentrated in different regions of sky in different observing runs and thus it is possible that poor, and epoch-dependent, instrumental residual removal could lead to apparent large scale alignments in different regions of sky. On the other hand, incorrect residual removal is very unlikely to mask real regions of aligned position angles as the errors would have to conspire in such a way as to randomize the observed position angles in regions of true alignment.

The analysis presented in Paper I leads us to believe that systematic errors in the residual calibrations are at a level $\sim 0.3\%$.

• *Polarization position angle calibration.* Errors in position-angle calibration would lead to position angles being systematically wrong, perhaps by different amounts in different observing runs. We believe that errors in the position angle calibration are at the level of $\leq 10^\circ$. Position-angle calibration errors cannot produce areas of systematic alignments where none exist. They could, however, reduce the prominence of areas of real alignment if the errors were large enough and changed systematically across a region of real alignment. But at $\leq 10^\circ$ these errors are small and, in fact, comparable to the random errors on the majority of sources. Thus they are not a good reason for missing real alignments.

• *Data analysis – CLEAN bias.* Even with perfect calibration it is possible for the analysis technique adopted to lead to systematic biases in the distribution of polarization position angles. In particular the CLEAN deconvolution process suffers from a tendency to bias flux densities towards zero by an amount that depends on the number of CLEAN iterations. For total intensity data this is relatively benign, but for the analysis of polarization data where Stokes Q and U maps are separately cleaned it can cause significant problems when Q and U are combined to give a position angle. This is because Q and U can be negative and because polarized flux densities are generally low. Hence biases towards zero are proportionately more significant and result in a disproportionate number of sources having apparent position angles around zero, $\pm 45^\circ$ and $\pm 90^\circ$. The issue of CLEAN bias and other systematic effects which may affect polarization measurements are discussed more extensively in Battye et al. (in prep). It is to avoid the effects of CLEAN bias that the results we analyse in this paper have all been obtained by model fitting in the visibility plane without the use of CLEAN.

2.2 Westerbork Data at 5 GHz

JVAS and CLASS were made using the VLA which has feeds that produce opposite hands of circular polarization that can then be cross-correlated to produce linear polarizations (Stokes Q and U). We thought it useful to check the accuracy of the VLA polarization results by comparing them with measurements obtained in a different manner. Also, if the measurements were done at a different frequency this would give some Faraday rotation information.(See Section 7) We therefore observed 340 sources from JVAS/CLASS lists with Westerbork Synthesis Radio Array (WSRT) at 5 GHz. This uses linear-polarization feeds to obtain the polarization information; thus the methodology is completely different from that of the VLA.

All the sources observed were within $0 \leq \delta \leq 40^\circ$, and had polarized flux density, $P \geq 4$ mJy at 8.4 GHz. Not all the measurements were successful and we obtained useful polarization data for 336 objects. Fig. 2 compares position angles (PA) from JVAS/CLASS and WSRT data; the difference clearly peaks at 0°.

Full details of the observations, their calibration and

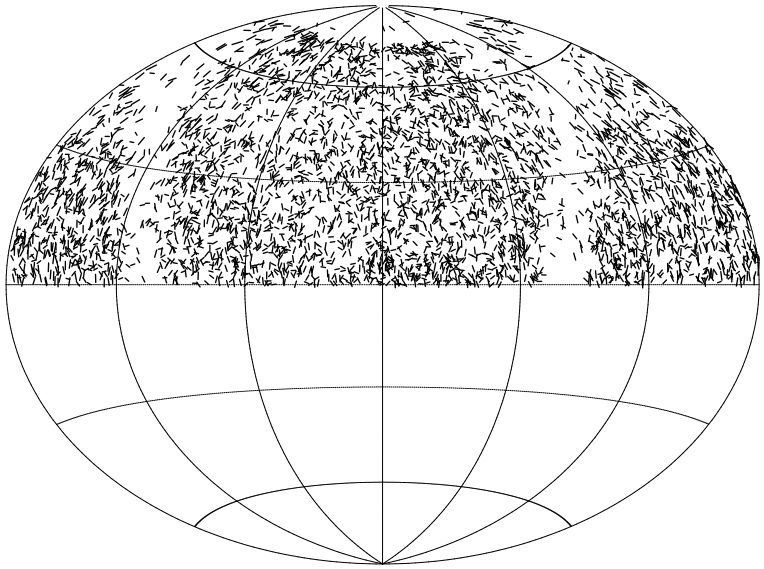

Figure 1. Aitoff plot for all the objects in the sample we used, from JVAS/CLASS samples. The lack of uniformity arises from the exclusion of low Galactic latitude sources from CLASS and the fact that in some CLASS regions we were not able to calibrate the polarizations to our satisfaction.

analysis will be given elsewhere (Joshi et al, in prep). Briefly, CTD 93 and 3C 286 were observed as flux and polarization calibrators. The data analysis was performed using the NEWSTAR package. The target sources were assumed to be point-like and the values for Stokes Q, U (and V) were obtained by model fitting.

3 STATISTICAL ANALYSIS

Our polarization data as described in Paper I have been analyzed for signs of statistical non-uniformity of the type claimed by Hutsemékers et al (2005). In Paper I it was shown that the distribution of position angles for the sample treated as a whole was consistent with uniformity. However, this does not preclude the possibility of sub-areas in which there are locally strong alignments. Four tests have been performed. In the first two the sky has been divided into "tiles" defined using the HEALPix software package (Górski et al., 2005) and the distribution within each tile has been tested for non-uniformity using a χ^2 test on the histograms and by adding the polarization vectors to form a random walk. In the third test a search has been made for clusters of aligned position angles using a nearest neighbour analysis. In the last test we implemented one of the approaches used by Hutsemékers et al. All these tests applied to the 4290 objects from JVAS and CLASS catalogues for which $P \geq 1$mJy.

3.1 Histogram method

We have investigated a simple adaptation of the histogram test performed on whole dataset in Paper I which is designed to search for localized non-uniform behaviour. The data were split up into pixels defined by the HEALPix software and the χ^2 of each of these histograms of position angles was computed on the assumption that the expected distribution was uniform. This value is then compared to the χ^2 found for 10000 realizations of sources at the same positions, but with PAs which are drawn from a uniform distribution. For the real data the number of pixels that have a χ^2 indicating that the distribution has failed the test for uniformity at different degrees of significance is noted. This is compared to the number one might expect for that number of pixels

The size of each pixel is defined by the HEALPix variable $n_{\rm side}$, which gives the number of pixels in the whole sky $n_{\rm pix} = 12n_{\rm side}^2$, and hence the area of a pixel is $\Omega_{\rm pix} = \theta_{\rm pix}^2 = 4\pi/n_{\rm pix}$. We also need to choose a bin size for the histogram which is defined by $n_{\rm bin}$, the number of bins covering the range -90° to 90°, which is varied in the analysis. Moreover, we have performed this test using two different coordinate systems (celestial and galactic) so as to investigate the effects of choice of pixel shape defined by HEALPix.

The results of this test are presented in Table 1 for $n_{\rm bin} = 4$ and the celestial coordinate system. For large pixel sizes ($\theta_{\rm pix} \approx 58.5^\circ$ and 29.3°) there is a slight excess of pixels which fail the test - one would expect around 5% of pixels to fail the test at 95% confidence, for example - and

$\theta_{\rm pix}$/deg	$n_{\rm obj}$	$N(95\%)$	$P(95\%)$	$N(99\%)$	$P(99\%)$
58.5	8	1	12.5	0	0
29.3	28	2	7.1	1	3.5
14.7	103	3	2.9	2	1.9
7.3	392	10	2.5	5	1.2
3.7	1342	7	0.5	1	0.07

Table 1. Results of the histogram test. $\theta_{\rm pix}$ is the approximate pixel size, $n_{\rm obj}$ is the number of pixels containing an object. $N(95\%)$ and $N(99\%)$ are the number of pixels which fail the test at 95% and 99% respectively, that is, those pixels for which the χ^2 is greater than that found in 500 and 100 of the random 10000 realizations, respectively. $P(95\%)$ and $P(99\%)$ quantify the number of failures as a percentage of the pixels containing a source.

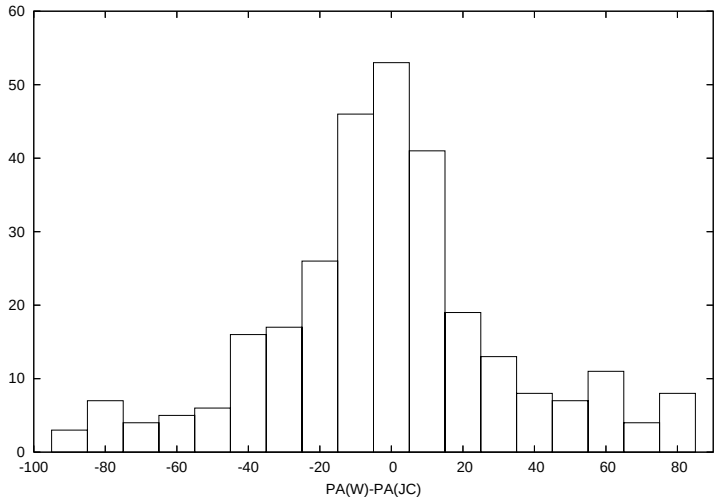

Figure 2. The histogram of the differences between position angles measured using the WSRT and the VLA in the JVAS/CLASS surveys.

substantially less failing than one expects for $\theta_{\rm pix} \approx 3.7^\circ$. The latter result can be understood by realizing that there are, on average, less than 5 sources per pixel in this case. The results for large pixel sizes can be "explained" as being due to small number statistics. For $\theta_{\rm pix} = 14.7^\circ$ and 7.3°, things seem compatible with there being no excess alignment, over and above that which is expected.

This test is however not completely robust since it relies on a choice of $n_{\rm bin}$ and the coordinate system. We have checked that the results presented in Table 1 are not particularly sensitive to these choices by using $n_{\rm bin} = 6$, and also a galactic based coordinate system. Hence, we conclude that the test is compatible with the null hypothesis that the PAs are chosen from a uniform distribution.

3.2 Random walk test

We have performed another test using the HEALPix-defined pixelation scheme: for each source in the pixel we have constructed a unit vector in the direction of the polarization ($\hat{p}_{\rm i} = (\sin 2\theta, \cos 2\theta)$) and these are then added together to form a random walk. Again the results are compared to 10000 realizations whose PAs are drawn from a uniform distribution. In contrast to the histogram test, this does not require the choice of $n_{\rm bin}$; it also seems to work better when there are smaller numbers of sources in the pixels. It does, however, still depend on a choice of coordinate system.

The results of this test are presented in Table 2. We see that again that there is a slight excess of pixels which fail the test for large pixel sizes, but that the number failing the test appears compatible with uniformity for lower values of $\theta_{\rm pix}$.

3.3 Nearest Neighbour Method

As a simple global test to see if the PA are aligned we used the following method: for every object, the n nearest objects are checked for alignment. If the object has PA within $\Delta\theta$ of the object under consideration, it is considered aligned.

$\theta_{\rm pix}$/deg	$n_{\rm obj}$	$N(95\%)$	$P(95\%)$	$N(99\%)$	$P(99\%)$
58.5	8	1	12.5	0	0
29.3	28	3	10.1	1	3.5
14.7	103	2	1.9	0	0
7.3	392	16	4.0	4	1.0
3.7	1342	56	4.1	7	0.5

Table 2. Results from the random walk test. The columns are the same as in Table 1

The choice of the appropriate value of n depends on the size of the sample, since the probability of finding n alignments by chance should be low. It also depends upon the scale of any real clustering in the data which is, of course, unknown. However, if the regions over which alignments occur contain more than n objects, the test will pick out many objects in the same area all of which will have significantly more rear neighbours having aligned polarizations than expected by chance and real structures will not be missed. We initially choose a value of $n = 25$ but have explored other values up to a maximum of $n = 250$. We typically used $\Delta\theta = 45^\circ$ since all the errors on the PA measurements are significantly smaller than this angle.

For the whole sample a histogram showing the number of objects having N out of 25 aligned nearest neighbours is plotted in Fig 3. The error bars have been derived from 5000 random realizations where, keeping positions of the objects the same, the sky was populated with sources having random PAs and the nearest neighbour test performed on each realization thus producing 5000 histograms like the one shown in Fig 3. For each bin in the histograms the distribution of values was obtained and fitted by a Gaussian. The plotted points and error bars are, respectively, the means and standard deviations obtained from the Gaussian fits. It is clear that, given the error bars, the real histogram is a reasonably good fit to that expected for a sample with randomly orientated position angles; the χ^2 for the real distribution when

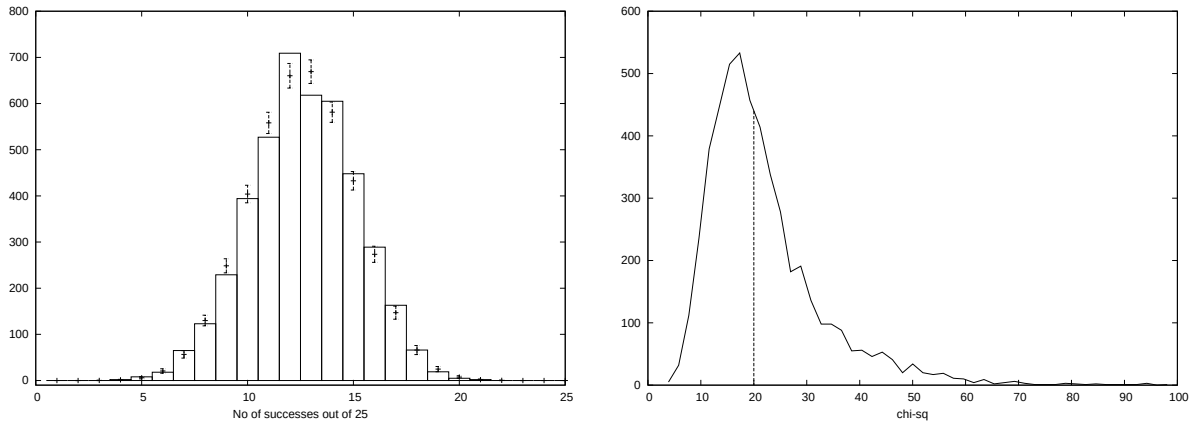

Figure 3. Comparison of nearest neighbour distribution for the 4290 JVAS/CLASS objects with that expected for a randomly oriented sample obtained from 5000 random realizations. The solid lined-histogram is for the real data and dashed data with error bars is from 5000 random samples. χ^2 for this distribution is 20.1. The right hand panel shows the distribution of χ^2 obtained by comparing each random realization with the averaged of all the random ones. The line represents χ^2 for the observed sky.

compared with the average random distribution is 20.1. The appropriate number of degrees of freedom is not obvious because the numbers in the histogram bins are not statistically independent. In Fig. 3b we show the distribution of χ^2, obtained from the random realizations, by comparing each with the mean of the 5000, with the line marking the χ^2 for the real sky. The probability of finding a χ^2 equal to or greater than the observed one is 45%.

3.4 Hutsemékers' test

Hutsemékers (1998) used a dedicated statistical test to identify if the polarization vectors are aligned in 2D or 3D space. It is more sophisticated than our own nearest neighbour test in that it gives extra weight to aligned objects according to their degree of alignment and distance apart. (See Hutsemékers (1998), Section 5.1 for the complete description.) As in our implementation of our nearest neighbour test, alignments were searched for within $\sim 45^\circ$ in groups of 25 objects. We have implemented the Hutsemékers (1998) test on JVAS/CLASS data in 2D (since we have incomplete redshift information). In this test, a parameter, S is calculated which depends upon the spatial distribution of objects, their PAs and the distribution of these. We find S = 68.6 for the 4290 sources in the JVAS/CLASS sample. To test whether or not this value of S indicates statistically significant clustering we generated 5000 random samples. For each sample the positions of the objects are same as those observed but PAs are randomized. The S distribution obtained from the random samples is shown in figure 4. Using this distribution we find that the probability of finding $S \geq 68.6$ occurring by chance is 19%.

4 DIVISION OF THE SAMPLE INTO REDSHIFT BINS

Hutsemékers et al. have found that the statistical significance of their alignments are enhanced if they divide their sample into low and high redshift bins. We do likewise for the JVAS/CLASS results in order to make as close as possible comparison with results of Hutsemékers et al. Out of 4290 objects, redshift information is available for 1273 objects. The redshifts are between 0.03 and 4.72, with median redshift of 1.24. Again, the same nearest neighbour test was performed on the two samples, and on 5000 random realizations keeping the object positions the same, and assigning the position angles randomly from a uniform distribution. The histograms with error bars are shown in Fig. 5, together with the distribution of χ^2. For the real sky, χ^2 values are 23.8 and 18.8 for low and high redshift regions, respectively. Values of these or greater have probabilities of occurrence as almost 1 in 2 and 1 in 4, in low and high redshift regions, respectively.

5 AN EXAMINATION OF THE HUTSEMÉKERS ET AL. REGIONS

Hutsemékers et al. claim that in different regions of sky quasar optical polarization position vectors are strongly aligned. In Fig 6 we plot the distribution of radio polarization position angles of our sources that are found within the regions identified by Hutsemékers et al. They defined regions A1 and A3 as, $168^\circ \leq \alpha \leq 218^\circ$ and $\delta \leq 50^\circ$, and $320^\circ \leq \alpha \leq 360^\circ$ and $\delta \leq 50^\circ$, respectively. We do not have any radio data for $\delta < 0^\circ$ so we do not have exactly the same area coverage as they do. No obvious alignments are visible on the sky or in the histograms of position angles also shown in Fig. 6. We have also performed our nearest neighbour test on the observed data in these regions and again produced 5000 random realizations as described above. The resulting histograms are shown in Fig. 7. The two regions have χ^2 of 34.1 and 28.3 respectively, with the probability of occurrence of a χ^2 greater than or equal to these values being almost 1 in 2 and 1 in 5, respectively. In contrast, our test applied to the optical data, showed a high significance detection of non-uniformity. The probabilities of the optical position angles being uniformly distributed are $\leq 0.7\%$ and

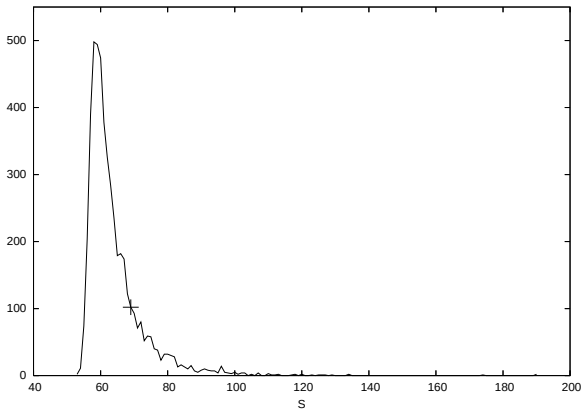

Figure 4. The distribution of the parameter S for 5000 random samples. For the observed data, S is 68.6 and is marked by a line in the figure.

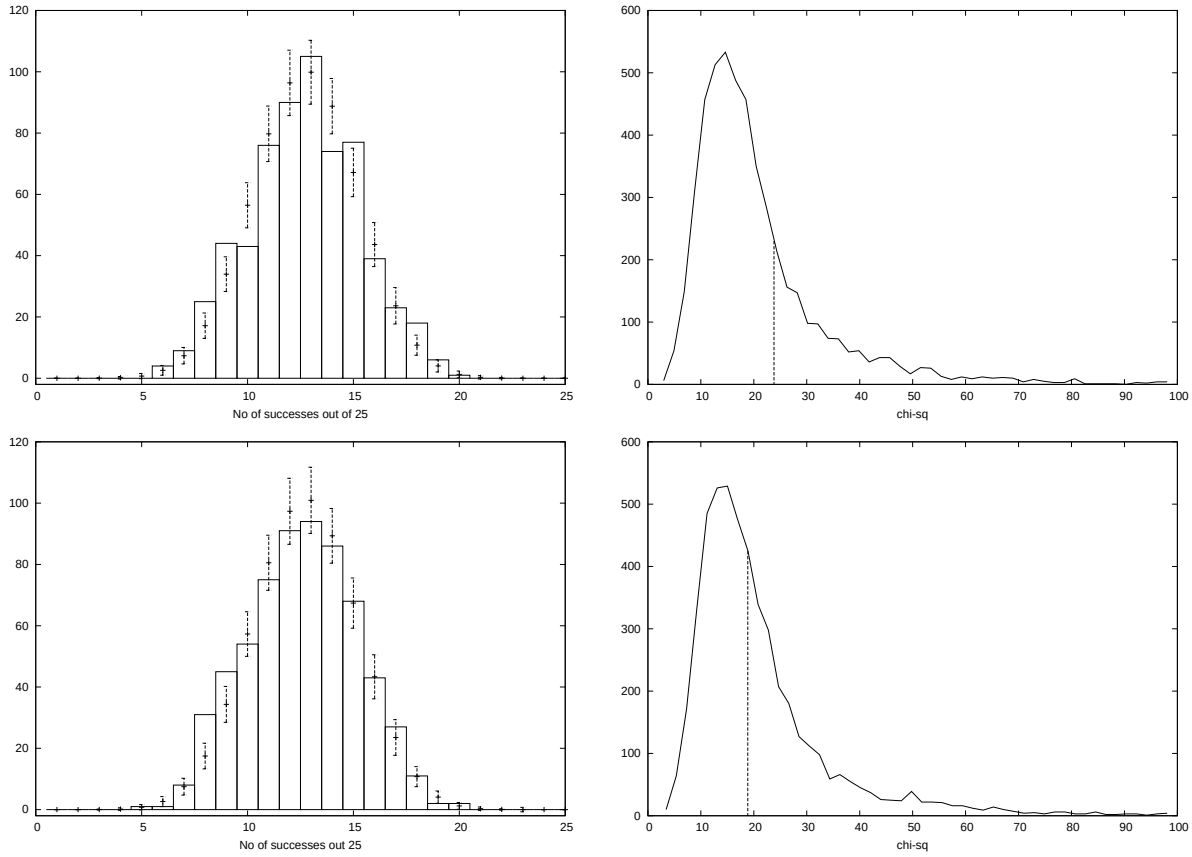

Figure 5. Histograms for low and high redshift samples. The panel on the top left shows histogram for objects with low redshift, the one at the bottom left is for high redshift objects. The solid line represents observed the data and dashed line is for random objects. The reduced χ'^2 for these two histograms are 0.26 and 0.29 respectively.

12%, for regions A1 and A3, are respectively[1] (See Fig. 7, panels at the bottom for region A1.)

Finally we compare the radio and optical position angles for objects common to JVAS/CLASS and Hutsemékers et al. The areas do not overlap completely as Hutsemékers et al., have analyzed the data for alignments near northern and southern galactic poles, whereas JVAS/CLASS surveys covered all RA ranges but only declination $\geq 0°$. We find 52 of their sources for which we have reliable polarization measurements at 8.4 GHz. (See appendix for the data.) Figure 8 shows the distribution of PA differences in optical and radio. There is no obvious correlation between the optical and ra-

[1] It should be noted that Hutsemkékers et al. preferentially targeted quasars in redshift slices where alignments had been previously suspected and thus the non-uniformity might be more prominent than in the radio where no redshift targeting was done.

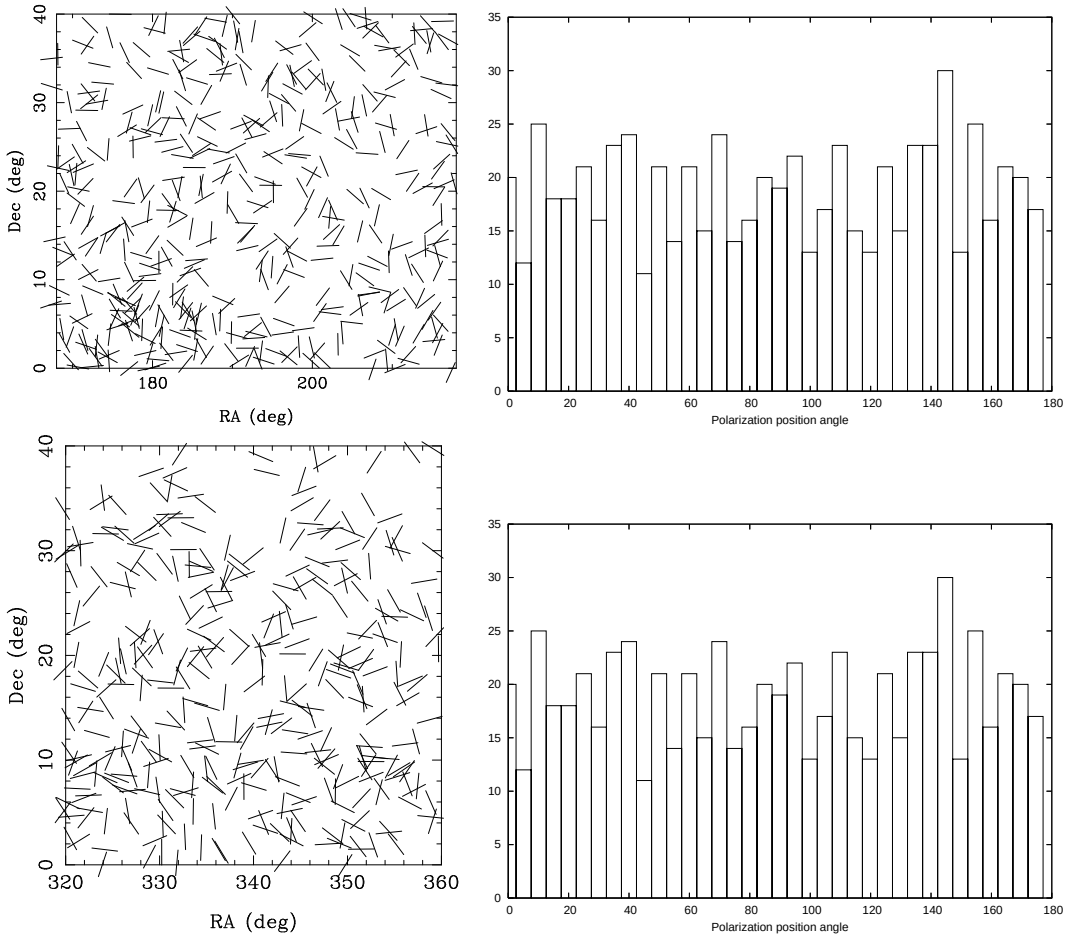

Figure 6. The left top panel shows flat-sky projection of the 8.4 GHz PAs in Hutsemékers et al. region A1, and the right hand panel shows histogram of the PAs. The bottom panels are the same for Hutsemékers et al. region A3.

dio polarization position angles. This is perhaps not surprising since correlations between radio and optical polarization position angles have been searched for in the past but none conclusively found (Lister & Smith (2000)). In summary, we find no evidence to suggest that there is anything special about the radio polarization properties of the objects found in the Hutsemékers et al. regions.

6 COMPARISON BETWEEN POLARIZATION POSITION ANGLES AND THE AXES OF PARSEC-SCALE JETS

Birch (1982) claimed that there were systematic offsets between radio polarization position angles and the direction of elongation of radio sources and that these were systematically correlated over the large regions. We have undertaken a similar investigation using our polarization position angle measurements and jet axes derived from VLBI maps. We use information on sub-kiloparsec scales rather than much larger scale information used by Birch because the majority of JVAS/CLASS objects, as a result of the spectral index selection used to define the sample, are compact with little observational information available on their structures on the scales of 10s to 100s of kiloparsecs. However, there is plenty of parsec-scale information. Using data from the literature (Beasley et al., 2002; Fomalont et al., 2003; Henstock et al., 1995; Kovalev et al., 2005; Petrov et al., 2005; Petrov et al., 2005; Kovalev et al., 2007; Polatidis et al., 1995; Taylor et al., 1994; Thakkar et al., 1995; Xu et al., 1995; Zensus et al., 2002) and that available in web-based archives we have estimated jet position angles for 1565 sources. There are 842 of these for which we also have polarization position angles. (See online data.) The jet position angle is defined to be in the range -180° to 180° measured from North through East. The position angles were measured by eye and we estimate the likely uncertainty of these measurements to be $\pm 10^\circ$.

The first thing to note is that the distribution of jet position angles is not uniform (see Fig. 9a). The two peaks at $\pm$ 90° arise because typical VLBI arrays have more resolution in the East-West direction than they do in the North-South direction. There is, therefore, a higher probability of being able to detect a measurable jet in the East-West direction than in the North-South. We note, however, that the distributions of jet angles should not depend on the areas of sky in which they are measured. The non-uniform overall distribution should not severely affect local statistics such as those employed in the earlier analysis of polarization position angles.

In order to investigate local correlations, we have done two things: we have examined the distribution of position

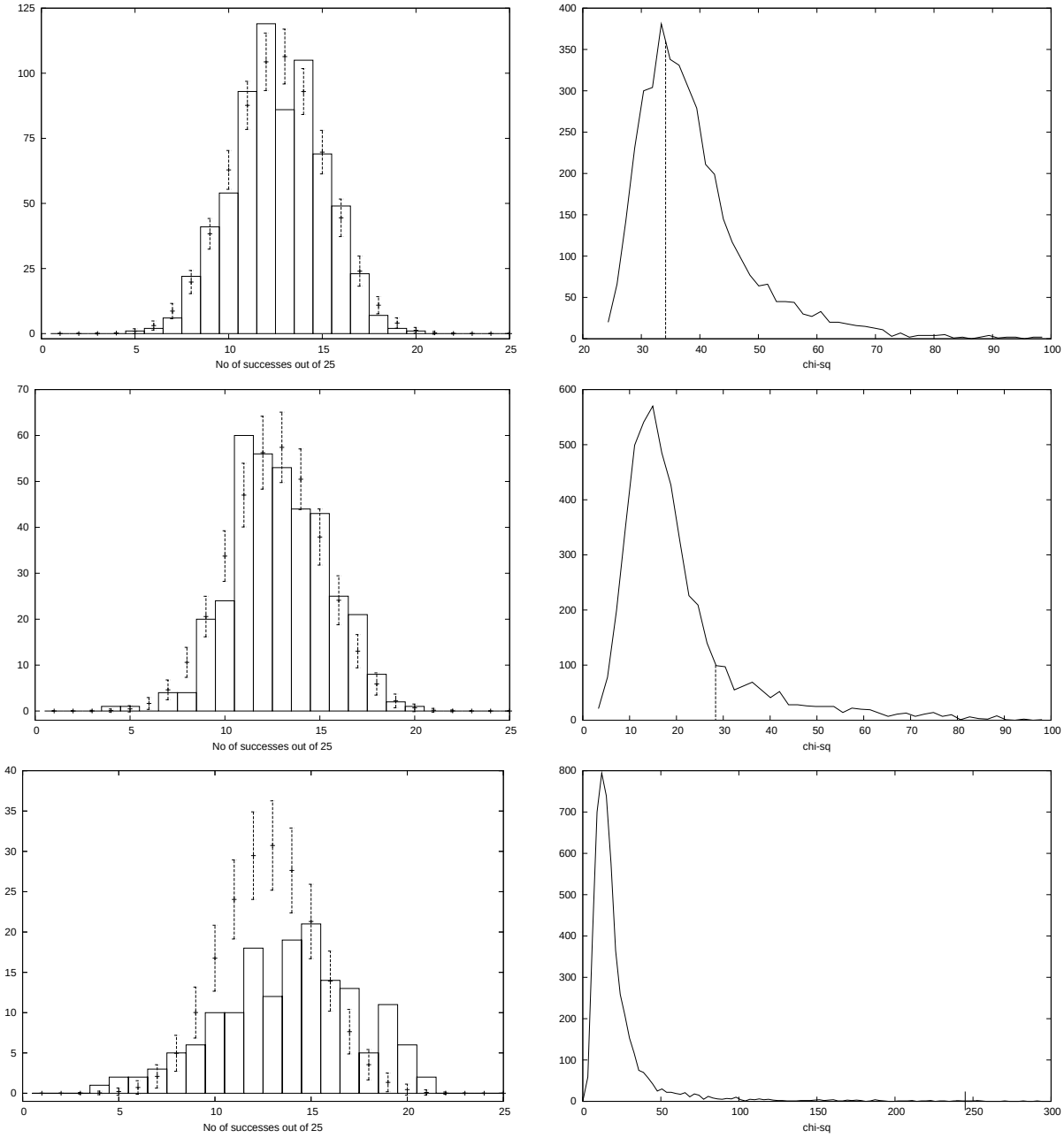

Figure 7. The left top panel shows the histogram from nearest neighbour test for region A1, with error bars from 5000 random realizations. The right top panel shows the χ^2 distribution for random realizations with the line showing that for the real sky in region A1. The middle panels show the same, for region A3. χ^2 for the region A1 is 34.1 and 28.3 for the region A3. The probability of finding this χ^2 or more is 52% for region A1 and that for region A3 18% respectively. The panels at the bottom are for region A1 again, but show the results for the optical data. For these χ^2 is 245 with probability of 0.7% under the hypthesis that the distribution of position angles is uniform.

angles to see if there are any systematic deviations from uniformity in different parts of the sky and we have looked at the polarization position angle/VLBI jet angle difference for any similar effects.

6.1 The distribution of jet position angles

We have performed the histogram and random walk tests on the data using $n_{\rm bins} = 4$ and the celestial coordinate system. The results are presented in Table 3. It is clear that for $\theta_{\rm pix} \leq 29.3^\circ$ the results are compatible with uniformity and the case of $\theta_{\rm pix} = 58.6^\circ$ is dominated by small number statistics.

We also have performed the nearest neighbour test on the jet angle data to look for regions of sky where there might be clusters of sources with aligned position angles. No obvious regions were found. From these three tests, therefore, we conclude that the jet angles show no tendency to align in different regions of sky.

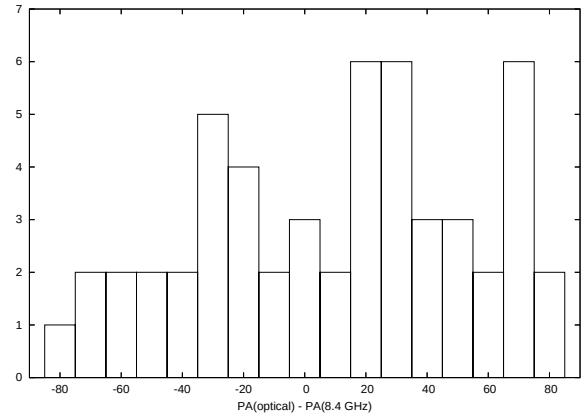

Figure 8. The PA difference distribution for 52 common sources in JVAS/CLASS survey and Hutsemékers et al (2005) sample of quasars.

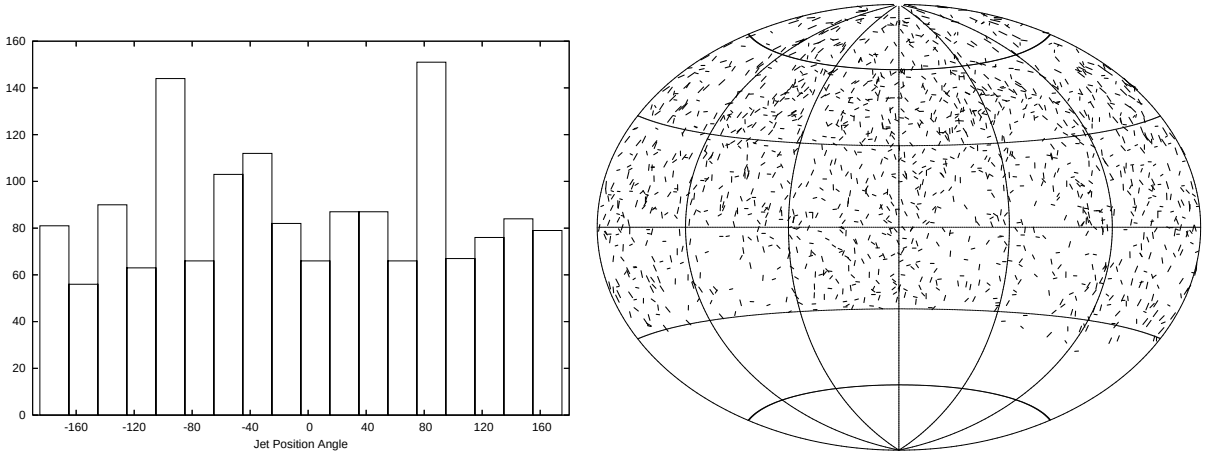

Figure 9. a) The left hand panel shows jet-angle distribution of 1565 sources. Two peaks at $\pm$ 90° stand out clearly. b) On the right hand is the Aitoff projection of distribution of jet PA on the sky.

6.2 Correlations between jet and polarization position angles

The histogram of the difference between jet PA and polarization PA is shown in Fig. 10. It is clear that there is a peak near 90° with a less significant peak around 0°. These 90° and 0° peaks are consistent with previous results (e.g. Gabuzda et al., 1994; Helmboldt, et al., 2007; Lister and Smith 2000; Pollack et al., 2002). Such a correlation is also expected on astrophysical grounds since the magnetic field vectors of the emitted radiation are known to align along the local jet direction or, less frequently, perpendicular to it (e.g. Gabuzda et al., 1992). The lack of uniformity in the polarization/jet position angle distribution, which survives the effects of resolution and selection involved in the construction of our sample, means that one needs to be careful when looking for signatures of systematic alignments. However, an obvious test is to look at the sign of the position angle difference for any evidence of an effect similar to that found by Birch (1982). We have done this using the nearest neighbour test where we define a 'success' as a neighbour having the same sign as the source in question and a failure, one having the opposite sign. The results of the test are displayed in histogram form in Fig 11. There is no evidence for regions having large numbers of either negative or positive position angle differences.

7 DISCUSSION

None of the statistical tests we have performed (see Section 3) indicate any areas in which there are large-scale alignments of PAs measured at 8.4GHz, in contrast to what has been found in the optical wavelengths by Hutsemékers et al. Could this be due to some error in the radio results arising from instrumental bias in PA measurement, or a data analysis error? We think this is highly unlikely because the data have been carefully re-analyzed paying particular attention to the polarization calibration and the extraction of the polarization parameters. External comparisons with other data, including our own Westerbork observations, convince us that CLASS polarization angles are reliable (See Section 2.2.)

We can think of two generic reasons why there might be alignments found in optical polarization position angles and not the radio ones:

- The physical mechanism that aligns the optical polarizations may be frequency dependent and not apply to the

$\theta_{\rm pix}$/deg	$n_{\rm obj}$	$N_{\rm hist}(95\%)$	$P_{\rm hist}(95\%)$	$N_{\rm rand}(95\%)$	$P_{\rm rand}(95\%)$
58.5	12	1	8.3	2	16.0
29.3	44	0	0.0	1	2.3
14.7	156	4	2.6	6	3.9
7.3	549	2	0.36	17	3.1

Table 3. Results of using the histogram and random walk tests on the jet position angle data. The first two results are the number and percentage of pixels which fail the histogram test at 95% and the second two are for the random walk test.

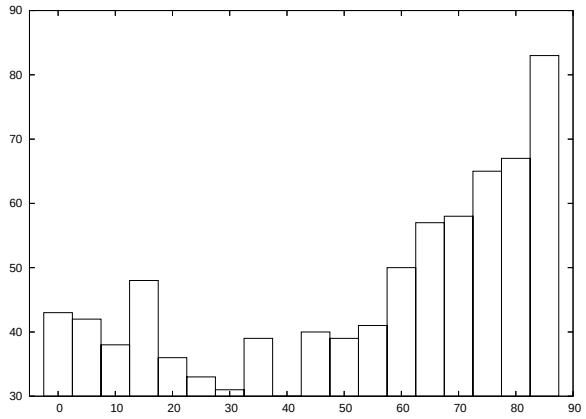

Figure 10. The histogram of difference between VLBI jet PA and polarization PA.

radio. This could either apply to the production of the radiation or any polarization imposed during propagation.

• The optical results could be misleading because of either statistical fluke or the polarizations are not primarily extragalactic in origin.

We first consider physical mechanisms. We have checked the optical sample of 355 quasars using Véron & Véron (2007) and the NASA Extragalactic Database (NED) and find that ∼72% are radio loud and most have flat radio spectra. Having a flat radio spectrum suggests that they are blazars and in blazars the optical and radio emission is predominantly synchrotron in origin. Thus for the majority of the radio and optical objects the radiation mechanism is the same and this argues against something intrinsic producing alignments detectable at optical wavelengths and not at radio wavelengths[2].

For radio-quiet quasars, the source of intrinsic optical polarization is likely to be scattering (Stockman, Moore & Angel (1984), Berriman et al (1990)). Perhaps significantly, the degree of alignment in radio-loud quasars and radio-quiet quasars cannot be distinguished statistically, though it should be noted that the radio-quiet sample is small. Thus, assuming the optical result is of cosmological significance, the more plausible explanation would be a propagation effect that polarizes optical emission and not the radio, or perhaps one that destroys the radio alignments. An obvious mechanism to destroy radio alignments is Faraday rotation. However, rotation measures would have to be of the order of thousands of radm^{-2} and this possibility can also be ruled out because:

• The rotation measures of extragalactic sources in general are normally quite low, often less than a few tens of radm^{-2} (e.g. Rudnick & Jones (1983), but see also Zavala & Taylor (2004) who measure very high rotation measure but on parsec scales). For JVAS/CLASS the random subset of objects for which we have measurements done at 8.4 GHz, 5 GHz (WSRT), and 1.4 GHz (NVSS) the rotation measures are around tens of radm^{-2} or less, rather than the order of thousands. (Joshi et al, in prep).

• There is a correlation between the position angles of radio jets and the corresponding magnetic field directions inferred from radio polarization measurements (Wills et al., (1992); Visvanathan & Wills (1998); Fig. 10 of this paper). Such a correlation would not be seen if the radio polarizations were significantly randomized by Faraday rotation.

We conclude that intrinsic mechanisms or Faraday rotation cannot account for the lack of radio alignments and therefore the most viable explanations are that either there is some, as yet uncertain, propagation effect that works on the optical photons and not the radio, or that the optical results have may not been interpreted correctly. This might be a result of the relatively small numbers alone or from the combination of small numbers and any residual biases in the data, perhaps caused by the effects of Galactic interstellar polarization. One suggestion discussed in Hutsemékers et al. (2005) is that radiation propagating over cosmological distances can be polarized by light weakly interacting pseudoscalar (or scalar) particles (Das et al, 2005) and that

[2] Despite the common radiation mechanism we and other authors do not find any clear correlation between the radio and optical position angles. We have 52 objects in common with Hutsemékers et al (see Section 5)

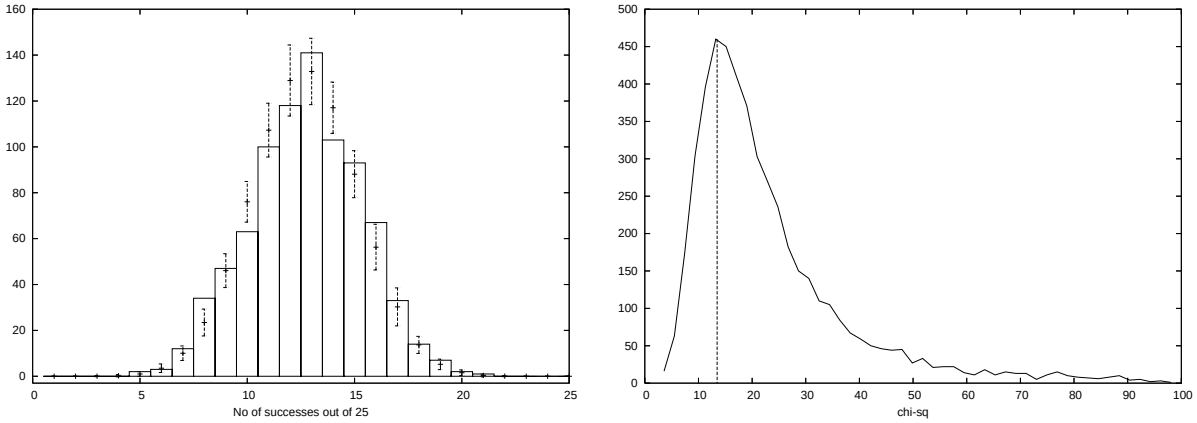

Figure 11. The left hand panel shows the results of the nearest neighbour test on differences between jet angles and polarization position angles. The right hand panel shows distribution of χ^2 with the real data having $\chi^2 = 13.5$, with probability of 69% of occurring under the hypothesis of a uniform distribution.

this propagation effect can be frequency-dependent. However, given the profound implications of a non-Galactic astrophysical origin for the observed optical result, and the absence of evidence for the equivalent effect seen in the radio, we remain unconvinced by the conclusions of Hutsemékers et al.

Finally, since there are models which predict that polarization PA could suffer small ($\sim 1^\circ$) systematic rotations on large angular scales (e.g. Skrotskii rotation produced by vector perturbations of a flat Friedmann-Robertson-Walker background described in Morales & Sáes, (2007)), we briefly address the question of whether or not in the future it might be possible to detect such small deviations from random alignments using radio polarization data. We suggest that the most promising approach would be to use the difference in PA between that of the polarization and that of parsec-scale jets measured with VLBI. The two are observed to be correlated with a dispersion of $\sim 30^\circ$[3] and only the polarization angles should be affected by the Skrotskii rotation. Approximately a thousand objects would be required to constrain the mean position angle at the degree level ($30^\circ/\sqrt{1000}$). To detect an effect, several regions containing the order of 1000 objects would be required. Thus, assuming no systematic errors, in samples of $\sim 10^4$ objects one would begin to be sensitive to alignments at the predicted levels. Already the number of objects with both polarization position angle measurements and jet measurements are significantly in excess of a thousand, so such tests of this type are beginning to be feasible and will be very powerful in the SKA era.

ACKNOWLEDGEMENTS

We thank numerous colleagues for advice, particularly Paddy Leahy and Simon Garrington. The National Radio Astronomy Observatory is a facility of the National Science Foundation operated under cooperative agreement by Associated Universities, Inc. The Westerbork Synthesis Radio Telescope is operated by the ASTRON (Netherlands Foundation for Research in Astronomy) with support from the Netherlands Foundation for Scientific Research NWO. This research has made use of the NASA/IPAC Extragalactic Database (NED) which is operated by the Jet Propulsion Laboratory, California Institute of Technology, under contract with the National Aeronautics and Space Administration. This work was supported in part by the European Community's Sixth Framework Marie Curie Research Training Network Programme, Contract No. MRTN-CT-2004-505183 "ANGLES". S.J. thanks the University of Manchester School of Physics and Astronomy for support.

[3] The smaller dispersion relative to the raw polarization position angles means that smaller samples would be required to detect an effect.

REFERENCES

Beasley, A.J., Gordon, D., Peck, A.B., Petrov, L., MacMillan, D.S., Fomalont, E.B., Ma, C., 2002, ApJS, 141, 13
Berriman G., Schmidt G.D., West S.C., Stockman H.S., 1990, ApJS, 74, 869.
Birch P., 1982. Nat 298, 451.
Browne I.W.A., Wilkinson P.N., Patnaik A.R. Wrobel J.M., 1998, MNRAS, 293, 257.
Browne I.W.A., Wilkinson P.N., Jackson N.J.F., Myers S.T., Fassnacht C.D., Koopmans L.V.E., Marlow D.R., Norbury M., Rusin D., Sykes C.M., 2003. MNRAS 341, 13.
Carroll S. M., and Field G. B., 1997, Phys. Rev. Lett., 79, 2349
Das, S., Jain, P., Ralston, J. P., Saha, R., 2005, JCAP, 6, 2
Eisenstein D. J., and Bunn E. F., 1997, Phys. Rev. Lett., 79, 1957
Falco E., Kochanek C. S., Munoz J. A., 1998, ApJ, 494, 47.
Fomalont, E., Petrov, L., McMillan, D.S., Gordon, D., Ma, C., 2003, AJ, 126, 2562
Gabuzda D.C., Rastorgueva E.A., Smith P.S., O'Sullivan S.P., 2005, MNRAS, 369, 1596
Gabuzda D.C., Mullan, C. M., Cawthorne, T. V., Wardle, J. F. C., Roberts, D. H., 1994, ApJ, 435, 140
Gabuzda D.C., Cawthorne, T. V., Roberts, D. H., Wardle, J. F. C., 1992, ApJ, 388, 40

Górski K.M., Hivon E., Banday A.J., Wandelt B.D., Hansen F.K., Reinecke M., Bartelmann M., 2005, ApJ, 622, 759
Helmboldt, J. F., Taylor, G. B., Tremblay, S., Fassnacht, C. D., Walker, R. C., Myers, S. T., Sjouwerman, L. O., Pearson, T. J., Readhead, A. C. S., Weintraub, L., Gehrels, N., Romani, R. W., Healey, S., Michelson, P. F., Blandford, R. G., Cotter, G. preprint (astro-ph/0611459)
Henstock, D. R., Browne, I. W. A., Wilkinson, P. N., Taylor, G. B., Vermeulen, R. C., Pearson, T. J., Readhead, A. C. S. 1995, ApJS, 100, 1
Hutsemékers D., 1998, A&A, 332, 410.
Hutsemékers D., Lamy H., 2001, A&A, 367, 381.
Hutsemékers D., Cabanac R., Lamy H., Sluse D., 2005, A&A, 441, 915.
Jackson N., Battye R. A., Browne I. W. B., Joshi S., Muxlow T. W. B., Wilkinson P. N., 2007, MNRAS, 376, 371.
Jain B., Scranton R., Sheth Ravi K., 2003, MNRAS, 345, 62.
Kendall D.. Young G., 1984, MNRAS, 207, 63.
Kovalev, Y. Y., Kellermann, K. I., Lister, M. L., Homan, D. C., Vermeulen, R. C., Cohen, M. H., Ros, E., Kadler, M., Lobanov, A. P., Zensus, J. A., Kardashev, N. S., Gurvits, L. I., Aller, M. F., Aller, H. D. 2005, AJ, 130, 2473
Kovalev, Y. Y., Petrov, L., Fomalont, E. B., Gordon, D., 2007, AJ, 133, 1236
Land K., Magueijo J., 2005, Phys. Rev. Lett., 95, 071301
Lister M.L., Smith, P.S. 2005, ApJ, 541, 66.
Lorado T. J., Flanagan E. E., Wasserman I. M., 1997, Phys. Rev. D, 56, 7507
Morales J.A, Sáez, D, 2007, preprint (astro-ph/0701914)
Myers S.T., Jackson N.J., Browne I.W.A., de Bruyn A.G., Pearson T.J., Readhead A.C.S., Wilkinson P.N., Biggs A.D., Blandford R.D., Fassnacht C.D., 2003. MNRAS 341, 1.
Nodland B., and Ralston J.P., 1997, Phys. Rev. Lett., 78, 3043
Patnaik, A. R., Browne, I. W. A., Wilkinson, P. N., Wrobel, J. M., 1992, MNRAS, 254, 655
Phinney E., Webster R., 1983, Nat, 301, 735.
Petrov, L., Kovalev, Y. Y., Fomalont, E., Gordon, D., 2005, AJ, 129, 1163
Petrov, L., Kovalev, Y. Y., Fomalont, E., Gordon, D., 2006, AJ, 131, 1872
Polatidis, A. G., Wilkinson, P. N., Xu, W., Readhead, A. C. S., Pearson, T. J., Taylor, G. B., Vermeulen, R. C., 1995, ApJS, 98, 1
Pollack, L. K., Taylor, G. B., Zavala, R. T., 2002, AAS, 201, 4817
Raeth C., Schuecker P., Banday A.J., 2007, preprint (astro-ph/0702163)
Rudnick L., Jones T.W., 1983, AJ, 88, 518.
Schwarz D.J., Starkman G.D., Huterer D., Copi C.J., 2004, Phys. Rev. Lett., 93, 1301S
Stockman H.S., Moore R.L., Angel J.R.P., 1984, ApJ, 279, 485.
Taylor, G. B., Vermeulen, R. C., Pearson, T. J., Readhead, A. C. S., Henstock, D. R., Browne, I. W. A., Wilkinson, P. N. 1994, ApJS, 95, 345
Thakkar, D. D., Xu, W., Readhead, A. C. S., Pearson, T. J., Taylor, G. B., Vermeulen, R. C., Polatidis, A. G., Wilkinson, P. N., 1995, ApJS, 98, 33
Véron-Cetty M.-P., Véron, P., A Catalogue of Quasars and Active Nuclei, 2007, 10th edition.
Visvanathan N., Wills B.J., 1998, AJ, 116, 2119.
Wardle, J. F. C., Perley, R. A., Cohen, M. H., 1997, Phys. Rev. Lett., 79, 1801
Wills, B.J., Wills D., Breger M Antonucci, R.R.J., Barvainis R., 1992, ApJ, 398, 454.
Wilkinson, P. N., Browne, I. W. A., Patnaik, A. R., Wrobel, J. M., Sorathia, B., 1998, MNRAS, 300, 790
Xu, W., Readhead, A. C. S., Pearson, T. J., Polatidis, A. G., Wilkinson, P. N., 1995, ApJS, 99, 297
Zavala, R.T, Taylor, G.B., 2004. ApJ, 612, 749
Zensus, J.A.,Ros, E., Kellermann,K.I., Cohen M.H., Vermeulen,R.C., Kadler, M, 2002, AJ, 124, 662

APPENDIX

RA HH MM SS	Dec DD MM SS	Name	I(8.4)	p%(8.4)	p%(op)	PA(8.4)	PA(op)	PA diff
00 27 15.374	22 41 58.17		320	0.378	0.63	151.3	90	61.3
01 08 38.771	01 35 00.32		2370	2.538	1.87	110.3	143	-32.7
01 21 56.862	04 22 24.75		1581	1.139	4.20	33.3	59	-25.7
01 26 42.791	25 59 01.28		869	2.743	1.63	155.7	140	15.7
03 39 30.938	-1 46 35.81		2801	2.894	19.40	121.0	22	81
04 23 15.801	-1 20 33.06		4383	1.959	11.90	99.6	115	-15.4
08 08 39.667	49 50 36.53		884	1.956	8.60	108.0	179	-71
08 41 24.366	70 53 42.17		1786	6.650	1.10	106.5	102	4.5
08 42 05.094	18 35 40.99		856	0.253	1.74	132.0	100	32
08 54 48.875	20 06 30.64	OJ 287	3907	2.530	10.80	79.9	156	-76.1
09 27 03.014	39 02 20.85	4C 39	8456	2.314	0.91	130.2	102	28.2
09 56 49.876	25 15 16.05		1903	0.270	1.45	37.2	127	-89.8
09 57 38.182	55 22 57.74		1447	3.141	8.68	2.2	4	-1.8
09 58 47.245	65 33 54.81		1276	9.601	19.10	159.5	170	-10.5
10 14 00.478	19 46 14.40		18	2.299	0.67	142.7	98	44.7
10 41 17.163	06 10 16.92		1359	0.864	0.62	109.8	149	-39.2
10 58 29.605	01 33 58.82		3853	1.217	5.00	122.4	146	-23.6
11 31 09.480	31 14 05.49		125	0.796	0.95	97.9	172	-74.1
11 59 31.834	29 14 43.83		1232	0.625	2.68	167.3	114	53.3
12 02 40.683	26 31 38.63		78	1.290	0.65	74.5	177	77.5
12 22 22.550	04 13 15.78		1045	0.901	5.56	87.5	118	-30.5
12 24 52.422	03 30 50.29		825	1.546	2.51	58.0	98	-40
12 24 54.461	21 22 46.43		1067	4.607	1.52	168.6	167	1.6
12 54 38.256	11 41 05.90		633	2.754	2.51	172.5	129	43.5
13 10 28.664	32 20 43.78		4029	2.577	12.10	11.6	68	-56.4
13 31 08.302	30 30 32.07	3C 286	2156	11.083	1.29	26.2	47	-20.8
13 43 00.180	28 44 07.50		196	0.254	0.81	175.6	45	49.4
13 49 34.656	53 41 17.04		742	1.884	1.73	78.2	161	-82.8
15 04 24.980	10 29 39.20		1772	2.207	3.00	179.1	160	19.1
15 24 41.612	15 21 21.06		335	4.557	7.90	90.2	32	58.2
15 34 52.454	01 31 04.21		930	1.417	3.50	151.7	131	20.7
15 40 49.492	14 47 45.90		833	3.438	17.40	156.0	145	11
15 50 35.270	05 27 10.46		1638	1.527	4.70	11.0	14	-3
15 58 55.185	33 23 18.61		106	0.645	1.31	37.7	70	-32.3
16 08 46.204	10 29 07.78		1767	1.792	2.10	54.5	134	-79.5
16 13 41.065	34 12 47.91		3197	5.430	1.68	5.0	134	51
16 35 15.493	38 08 04.50		2511	0.681	2.60	65.5	97	-31.5
16 38 13.456	57 20 23.98		1355	2.031	2.40	125.7	170	-44.3
16 42 58.810	39 48 37.00	3C 345	5653	4.220	4.00	24.8	103	-78.2
16 42 07.849	68 56 39.76		1254	3.933	16.60	154.0	8	34
16 57 20.709	57 05 53.51		517	2.814	1.34	157.6	51	73.4
17 23 20.797	34 17 57.99		213	2.290	0.74	111.6	143	-31.4
17 40 36.979	52 11 43.41		1357	1.174	3.70	21.1	172	29.1
17 48 32.841	70 05 50.77		573	3.404	11.50	91.8	112	-20.2
21 23 44.518	05 35 22.10		1539	2.679	10.70	64.0	68	-4
21 48 05.459	06 57 38.61		8042	0.557	0.60	70.0	138	-68
22 32 36.409	11 43 50.89	CTA 102	3029	1.290	7.30	89.0	118	-29
22 50 25.343	14 19 52.03	3C 4543	591	2.854	1.39	100.8	75	25.8
22 53 57.748	16 08 53.56		11031	2.377	2.90	5.3	144	41.3
22 54 09.342	24 45 23.47		456	5.593	1.34	44.1	113	-68.9
22 57 17.564	02 43 17.51		285	1.261	1.67	21.9	2	19.9
23 04 28.292	06 20 08.32		329	2.654	3.69	108.5	163	-54.5

Table 4. The 52 common objects in JVAS/CLASS surveys and Hutsemékers et al (2005) sample. Position information is from JVAS/CLASS data. I(8.4) stands for total flux at 8.4 GHz in mJy, p%(8.4) stands for percentage polarized flux at 8.4 GHz, p%(op)stands for percentage polarized flux in optical and PA(op) and PA(8.4) stand for polarization position angle in optical and at 8.4 GHz respectively. PA diff = PA(op)-PA(8.4).